Indian Journal of Advances in Chemical Science

Research Article

Hydrothermal synthesis, Characterization, DFT study, and Hirshfeld Surface Analysis of (2,2'-bipyridine)-bis (1,2,2-trimethyl cyclopentane-1,3-dicarboxylato)-copper (II) hydrate

Anupam Datta[1], Kanak Roy[1], Biswajit Sinha[2], Abhinath Barman[1], Subhra Mishra[3], Vikas Kr. Dakua[1], Mahendra Nath Roy[2]

[1]Department of Chemistry, Alipurduar University, Alipurduar, West Bengal, India, [2]Department of Chemistry, University of North Bengal, Darjeeling, West Bengal, India, [3]Department of Chemistry, Kharagpur College, Kharagpur, West Bengal, India

ABSTRACT

Copper (II) complex of 2,2'-bipyridine and D-camphoric acid, $Cu(C_{30}H_{38}O_8N_2)$ H_2O (I), was prepared and characterized by thermal analysis, and SCXRD determined the crystal structure. The title complex I crystallizes in tetragonal system, P41212, having crystallographic parameters, a = 21.21(16) Å, b = 21.21(16) Å, c = 7.01(5) Å, V=3156.6 (4) $Å^3$, and adopts a distorted octahedral geometry. A DFT study and Hirschfeld topology analysis of the complex (I) were also conducted. These studies revealed that the same achieves its three-dimensional structure and stability through O–H·O hydrogen bonding and the π-π stacking interactions between aromatic 2,2'-bipyridine rings.

Key words: DFT, Hirschfeld topology, Hydrothermal synthesis, SCXRD.

1. INTRODUCTION

The diversification in size, composition, charge, and structure of metal-organic frameworks led to numerous properties such as redox, catalytic, and magnetic, and has been receiving considerable current attention. The strong metal-chelating property of such coordination complexes has potential applications in biology [1,2]. As the properties of the complexes are dictated primarily by the coordination environment around the metal center, complexation of metal by ligands of selected types has been of significant importance, and the present work has originated from our interest in this area. For the complexation of copper, 2,2'-bipyridine and D-camphoric acid have been chosen as the ligand in the present study. It is well known that 2,2'-bipyridine has good chelating capacities as a bidentate, N, N-donor, forming a stable five-membered chelate ring [3]. It may be expected that this metal complex(I) has an interesting effect on the redox property and important applications in the biological field. The main objective of the present work has been to synthesize the mixed ligand complex of copper (II) and to study its structural properties. Among the many synthetic routes, hydrothermal synthesis has a large number of advantages over other types of crystal growth processes because this synthetic reaction does not require any catalyst and does not consume a large amount of time. However, the crystal formation depends on the types of ligands, the nature of metal salts, reaction temperature, and pH. This work mainly concerns the DFT study, Hirshfeld surface analysis, thermogravimetric analysis, and the crystal structure of this complex. Some authors have also reported similar types of this complex [4].

2. EXPERIMENTAL SECTION

2.1. Materials and Methods

D-Camphoric acid (99%), 2,2'-bipyridine (99.5%), and (Cu $[NO_3]_2 \cdot 3H_2O$, 99%), Sigma-Aldrich of A. R. grade chemicals were used without further purification. SCXRD studies were done using a Bruker AXS Kappa Apex 2 CCD diffractometer with a graphite monochromator with Mo *K*a (*k* = 0.71073 Å). Thermal analysis (TGA) was also done (under nitrogen flow~ 20 mL/min) using a Perkin Elmer Diamond TGA/DTA STA 6000, with a 2°C·min−1 scan rate.

2.2. Preparation of $Cu(C_{30}H_{38}O_8N_2)$ H_2O (I)

D-Camphoric acid (0.2005 g), 2,2'-bipyridine (0.1560 g), and Cu $(NO_3)_2 \cdot 3H_2O$ (0.2416 g) were refined and poured into a 10 mL Teflon autoclave, followed by the addition of 20 drops of 0.05(N) NaOH solution, and then 5mL of distilled water was added. The resultant mixture was stirred for 30 min to get a homogeneous suspension and then kept in an oven at 140°C/72 h. The autoclave was kept for 12 h at normal temperature. Translucent blue, block-shaped crystals were obtained. Yield: 70% based on the metal precursor. The crystal was insoluble in DMSO, DCM, CH_3CN, CH_3OH, DMF, and CCl_4 but was soluble in hot water, and the melting point was more than 300°C.

2.3. X-ray Crystallographic Measurements

For crystallographic studies, a Bruker Smart Apex II X-ray Single Crystal Diffractometer was used with graphite monochromator Mo Kα radiation (k = 0.71073 A°). The structure was refined and solved using SHELXL-97 and SIR 92, for data reduction and cell

***Corresponding Author**
Dr. Vikas Kumar Dakua
E-mail: dakuavikas7@gmail.com

ISSN NO: 2320-0898 (p); 2320-0928 (e)
DOI: 10.22607/IJACS.2025.1304004

Received: 14th November 2025;
Revised: 13th December 2025;
Accepted: 14th December 2025;
Published: 03rd January 2026

refinement, SAINT/XPREF and APEX2/SAINT programs were used, respectively. Mercury, SHELXL-97, and ORTEP 3 were utilized for computing molecular graphics [5-9]. The atoms other than H atoms were anisotropically refined, and all H atoms were placed in a Fourier difference map. The crystallographically refined data for complex I are given in Table 1, and selected bond angles and bond lengths are shown in Table 2.

2.4. Theoretical Study

DFT studies have been carried out to get an idea of the electronic structure of the title complex I and the same was refined with meta-hybrid TPSSh functional [10], and relativistic basis set executed through ZORA [11], retaining one-center terms and using ZORA-re-contracted def2-TZVP basis sets for all elements other than C and H, for which ZORA-def2-SVP basis sets were used [12]. To erase the inaccuracy, the resolution of identity, chain-of-spheres (COSX) approximations to Coulomb, and exact exchange, a large decontracted SARC/J auxiliary basis set was used [13,14]. Non-covalent interaction was figured out using atom-pairwise dispersion corrections with Becke–Johnson (D3BJ) damping [15]. All the calculations were executed in ORCA (version 5.3.0) [16]. The energies of the selected orbitals were taken from the quasi-restricted orbitals. The electrostatic potential (ESP) map or plot was obtained using the Gaussian 16, Revision A.03 program package. The DFT method used for the ESP plot includes the combination of B3LYP hybrid functional/LANL2DZ basis sets [17] for Cu (II) ion and a 6–31++g (d, p) double zeta basis set for the ligand atoms, respectively. The Crystal Explorer 17.5 program software has been used for molecular Hirschfield surface analysis to realize the crystal packing behavior and estimate the nature of interactions in molecular crystals [18].

Table 1: Crystallographic details

SCXRD Values of Complex I	SCXRD Parameters Complex I	
Chemical formula	$C_{30}H_{40}CuN_2O_9$	
M_F	636.18	
Temperature (K)	296 (2)	
Crystal system, space group	Tetragonal, P41212	
a, b, c (Å)	21.21 (16), 21.21 (16), 7.01 (5)	
V (Å^3)	3156.6 (4)	
Z, D_{cal}/(mg/m^{-3})	4, 1.364	
α=β=ϒ (deg)	90	
Radiation type	MoK\a	
Wavelength(Å)	0.71073	
F (000)	1372	
Absorption coefficient	0.749 mm^{-1}	
Crystal size	0.10×0.05×0.03 mm	
Limiting indices	-30<=h<=29, -30<=k<=28, -10<=l<=10	
Reflections collected/unique	48735/4912,	
Absorption correction	“Multi-scan”	
T_{max}, T_{min}	0.956, 0.978	
Restraints/parameters	1/199	
Goodness-of-fit on F^2	1.107	
Final R indices [I>2σ *(I)*]	R1=0.0599,	wR2=0.1274
R indices (all data)	R1=0.0413,	wR2=0.1048
CCDC	2143886	

3. RESULTS AND DISCUSSION

3.1. Structure of I, Cu($C_{30}H_{38}O_8N_2$) H_2O (I)

The SCXRD studies show that the title complex I has the molecular formula $C_{30}H_{40}CuN_2O_9$ and crystallizes in a tetragonal crystal system (P41212), and $Z = 4$. Here, the two bridging D-cam^{2-} ligand, bidentate 2,2’-bipyridine ligand, with Cu (II) ion form a distorted octahedral geometry shown in Figure 1. The Cu (II) ion was in the crystallographic center, the Cu (II) ion bound to two nitrogen atoms (*N*1, *N2*), from one 2,2’-bipyridine ligand and bound to two Oxygen atoms ($O1_a$, $O1_b$) from two different bridging D-cam^{2-} ligands, in a planar fashion in the equatorial plane at the distances of 1.954 A˚(16) for *Cu1- O1*and at the distances of 2.017(18) A˚ for Cu1–N1 and Cu1–N2, which were comparable to those of Hexaaza-macrocycle Cu (II) complexes with Cu–N distances in the range of 1.985(7)–2.017(6) A˚ [19,20]. In the axial plane, copper (II) ion bound to two oxygen atoms ($O2_a$, $O2_b$), again from two different bridging D-cam^{2-} ligands, at a distance of 2.600(19) A˚ which was significantly longer than those to the oxygen atoms in the equatorial position, however, slightly longer than Cu–O distances in the equatorial plane. This was due to the Jahn-Teller distortion of the Cu (II) ion in the z-axis with the elongation of the Cu–O bonding [21-23]. The geometry of the copper (II) ion for this complex could be described as a distorted octahedral geometry, like those reported complexes [19,20]. It was evident that the weakly non-coordinated water molecules were found outside the coordination sphere. Figure 2 shows the packing array of the title complex I furthermore all D-cam^{2-} ligands bind the metal centers with two different oxygen atoms (*O3/O1)* in a bridging fashion to form a unique Cu (II) binuclear unit forming tetragonal clusters, which are found to be stabilized by the aromatic □-□’ s stacking interactions as described by Lapshin [24].

3.2. TGA

The thermal resistance of complex I is studied and is shown in Figure 3. It has three stages, indicating the removal of different ligands from the metal ion with temperature rise. The initial mass loss from around 100 to 150°C may be assigned to weakly uncoordinated water molecules, followed by a sharp or steep weight loss stage at around 200 to 280°C, which is likely due to the removal of two bridging D-cam^{2-} ligands. Finally, the last stage, at around 300 to 570°C and more, is in all likelihood due to the removal of the coordinated 2,2‘-bipyridine fragment. The TGA curve remains unchanged in the 620–700°C temperature range corresponding to the metal oxide. Thus, we can conclude that complex I has appreciable thermal resistance at room temperature to relatively high temperatures, it was stable at 150°C, and thereafter it suffers step-by-step continuous thermal degradation up to 750°C to metal oxide residue.

Table 2: Selected bond lengths [Å] and angles [°]

Cu (1)- O (1)	1.9544 (16)	Cu (1)- N (1)	2.0170 (18)
Cu (1)- O (2)	2.6000 (19)	Cu (1)- N (2)	2.0170 (18)
N (1)- C (5)	1.341 (4)	N (1)- C (1)	1.351 (4)
O (1)- Cu (1)- N (1)	93.74 (8)	N (1)- Cu (1)- N (2)	81.09 (12)
O (1)-Cu (1)-N (2)	174.20 (7)	C (15)-O (3)-H (5) A	109.5
C (5)- N (1)- Cu (1)	126.14 (18)	C (1)- N (1)- Cu (1)	114.42 (18)
N (1)- C (1)- C (2)	120.7 (3)	C (3)- C (2)- C (1)	119.2 (3)

Table 3: Computed values of ionization potential (*I*), Electron affinity (*a*), Chemical potential (μ), Global Hardness (*η*), Global softness (*S*), and Electronegativity (*σ*). All the values are given in units of electron volt (eV)

Ionization potential (*I*)	Electron affinity (*a*)	Chemical potential(μ)	Global Hardness(*η*)	Global softness (*S*)	Electronegetivity (*σ*)
6.952	2.710	−4.831	2.121	0.471	4.831

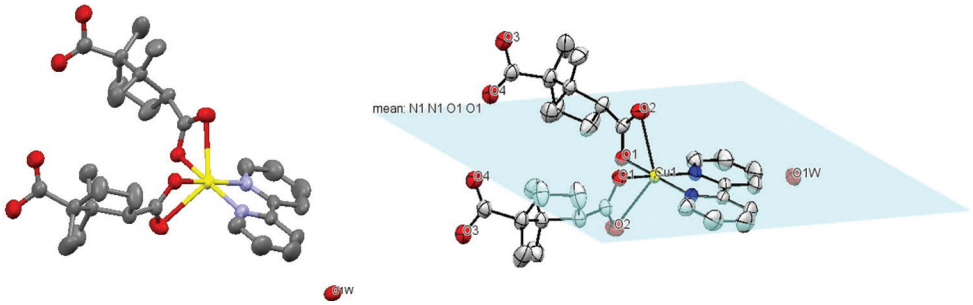

Figure 1: Distorted octahedral complex I. color scheme blue, N; red, O; Yellow, Cu; and gray, C.

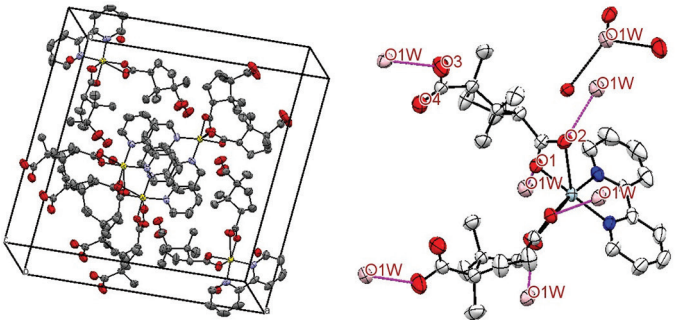

Figure 2: Packing diagram of the complex I within the unit cell and the hydrogen bonds within the complex.

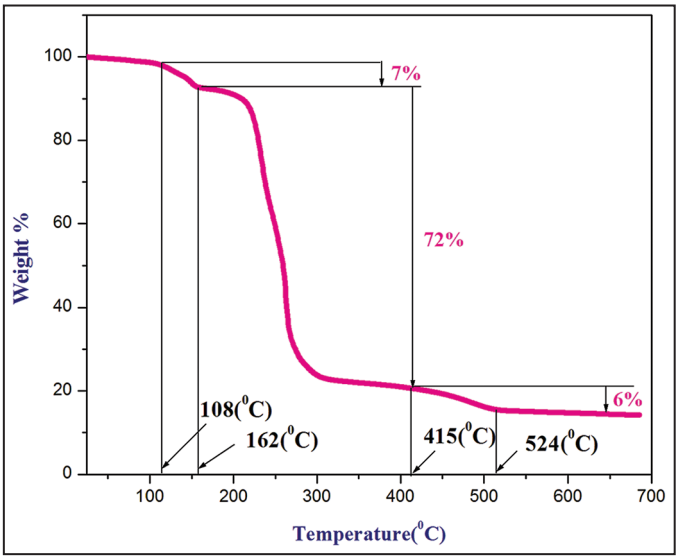

Figure 3: Thermal analysis curve.

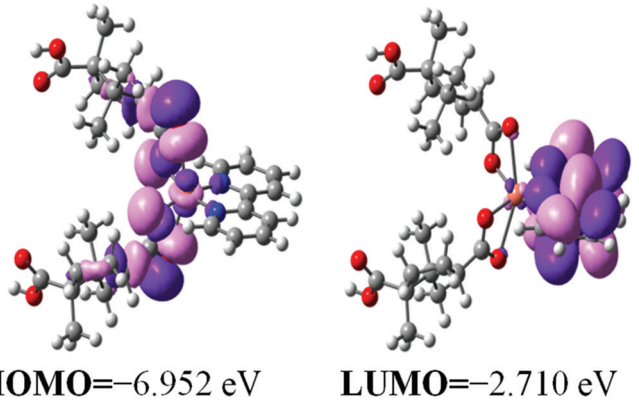

Figure 4: Optimized geometry and HOMO-LUMO of the synthesized complex I. H's attached to C- atoms are skipped for simplicity. Color code: Orange-Cu, Blue-N, Red-O, Gray-C.

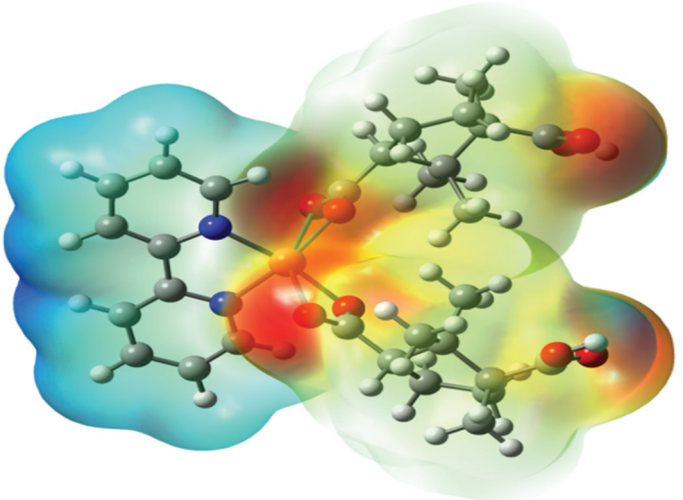

Figure 5: MESP diagram of the Cu (II) complex 1.

3.3. DFT Study

The complex's Cu (II) ion is located on a crystallographic inversion center, and two D-cam^{2-} ligands coordinate it, and one 2,2'-bipyridine ligand in an alternative way occupied axial and equatorial planes to form a distorted octahedral geometry. The energy gap between the highest occupied molecular orbital and the lowest unoccupied molecular orbital (HOMO-LUMO) was calculated using Gaussian 16.

The negative value of the energy of HOMO is directly related to the ionization potential of the ligand-metal complex, but electron affinity can be calculated from the energy of LUMO of the complex and are shown in Figure 4. The energy gap between HOMO and LUMO of a complex can be correlated with its stability. In addition, 3D plots

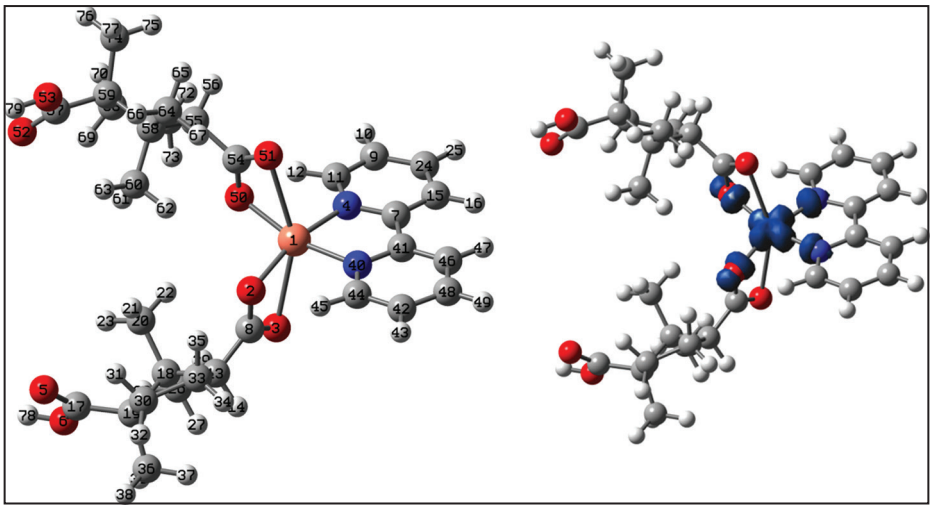

Figure 6: DFT optimized structure and Spin density of complex I.

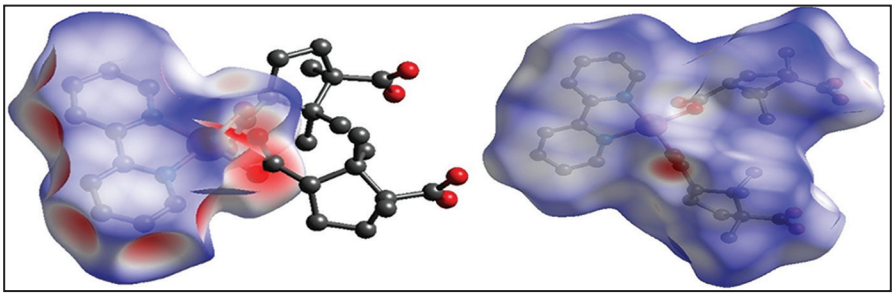

Figure 7: Molecular Hirschfeld surface: d norm.

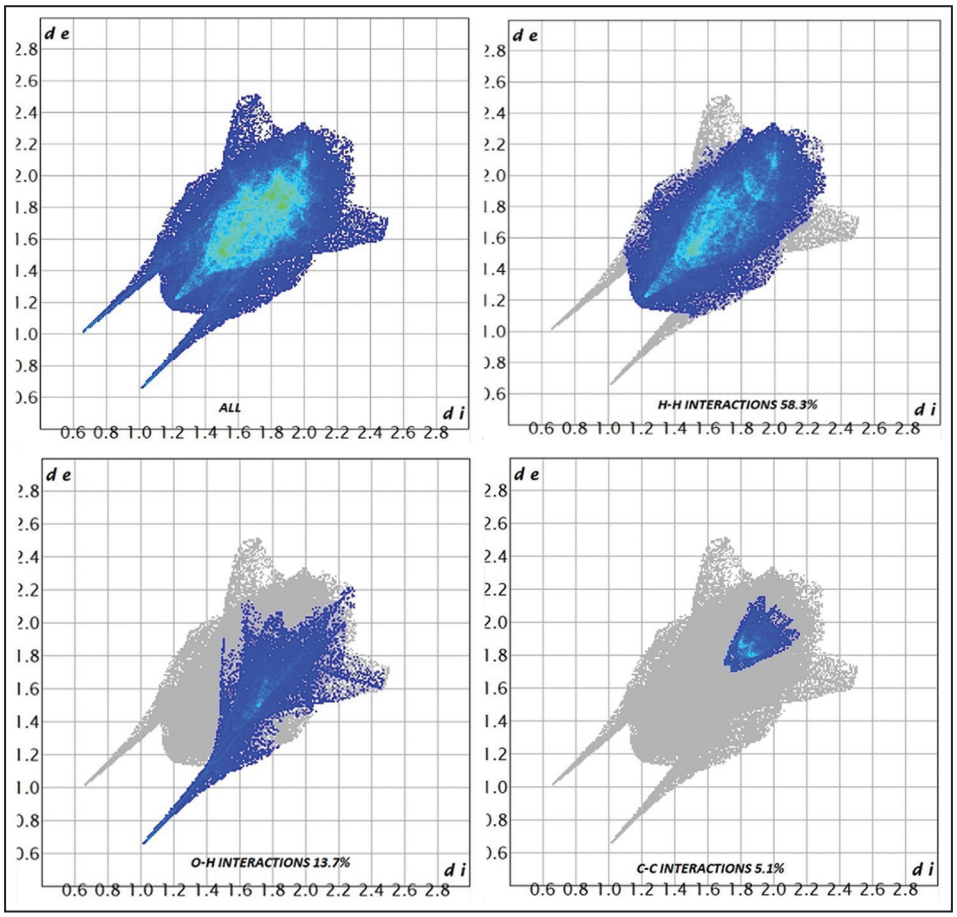

Figure 8: Fingerprint plots of complex 1 showing various elements' interactions in percentage.

of the HOMO and lowest unoccupied molecular orbital (LUMO) and spin density are shown in Figure 5. The energy of HOMO and LUMO has been calculated and found to be −6.952 and −2.710 eV, respectively, and the ΔE = (E_{LUMO}-E_{HOMO}) for the same is found to be 4.242 eV, indicating that the complex I is stable [25]. The DFT-based descriptors are used to calculate different theoretical physical parameters such as chemical potential (μ) = (E_{HOMO} + E_{LUMO})/2, global hardness (η) = (-E_{HOMO} + E_{LUMO})/2, global electrophilicity power (ω) = μ2/2η, ionization energy (I = - E_{HOMO}), and electron affinity (A = - E_{LUMO}), [26]. The negative value of μ of the above complex I indicates its thermal resistivity, air stability, and does not decompose continuously into its elemental form. The values of global chemical reactivity descriptors (*I, a, ∝, η, S, σ, and ω*) were evaluated using the above equations, which are given in Table 3. ESP maps at the B3LYP/LANL2DZ refined geometry were calculated and used to determine the potential nucleophilic reactivity (blue region), potential electrophilic reactivity (red, orange, and yellow regions), and hydrogen bonding interactions prevailing in the molecules [27-29]. The ESP map (MESP) of the title complex I is shown in Figure 5. Here, the oxygen atom of the carboxylic group, water, and hydroxyl group are assigned to the electrophilic reactivity sites, whereas the C and H atoms of the complex I bear nucleophilic reactivity region, and it was evident that the most reactive part of complex I is the carboxylic group due to the oxygen atom's electronegativity.

3.4. Hirschfeld Surface Analysis

This is a computable method for predicting the intermolecular interactions in a crystal structure. Hirshfeld surfaces and 2D fingerprint plots were graphed with Crystal Explorer 17.5 software [18]. The above analysis was realized by the d_{norm}, which was computed with the following equation,

$$d_{norm} = \frac{\left(d_i - r_i^{vdW}\right)}{r_i^{vdW}} + \frac{\left(d_e - r_e^{vdW}\right)}{r_e^{vdW}}$$

Where d_{norm} = normalized contact distance

d_e = Distance between the nearest nucleus (external) and Hirshfeld surface,

d_i = distance between the nearest nucleus (internal) and Hirshfeld surface, and r_i^{vdw} and r_e^{vdw} are the van der Waals radii of atoms. [30,31].

The Hirschfeld surface for the complex I; d_{norm} is presented in Figure 7 and graphed over ranges −0.7210–1.6048 Å. The parameter d_{norm}, normalized contact distance, shows the surface with bright red spots indicating close contact between neighboring atoms and white-blue spots devoid of close contacts, respectively. The computable determination of all possible intermolecular contacts is presented in Figure 8. It is clear that the H……H (*58.30%*), O……H (*13.70%*), and C……C (*5.10%*) contacts are prominent intermolecular interactions, which reveal that there are concordant relationships between these different color spots and molecular interactions.

4. CONCLUSION

The newly reported distorted octahedral Cu (II) complex is a blue, block-shaped, and tetragonal crystal, space group P41212. The π-π stackings were further interconnected through the hydrogen bonding interactions to give the same 3D supramolecular architecture. Hirshfeld analysis reveals that the crystal packing behavior of the above complex was controlled primarily by van der Waals interactions. Thermogravimetric studies and computational quantum mechanical modeling studies revealed its thermal stability.

5. ACKNOWLEDGMENTS

We are thankful to the Department of Chemistry, University of North Bengal, West Bengal, India, for financial support and also grateful to SAIF, Gauhati University, Assam, India, for carrying out TGA and SCXRD.

6. SUPPLEMENTARY DATA

Crystallographic data for complex I have been deposited to the Cambridge Crystallographic Data Center (CCDC), 12 Union Road, Cambridge CB2 1EZ, UK, CCDC-2143886.

REFERENCES

1. A. Kamath, G. Pilet, A. Tamang, B. Sinha, (2020) [{Diaquo(3,5-dinitrobenzoato-κ1O1)(1,10-phenanthroline-κ2N1:N10)} copper(II)] 3,5-dinitrobenzoate: Hydrothermal synthesis, crystal structure and magnetic properties. ***Journal of Molecular Structure***, **1199**, 126933.
2. P. Ristic, M. Rodic, N. Filipovic, (2021) Structural study of Pt(II) and Pd(II) complexes with quinoline-2-carboxaldehyde thiosemicarbazone, ***Journal of the Serbian Chemical Society***, **86(4),** 393.
3. A. Y. Fu, D. Q. Wang, (2005) Tris(pyridine-2-carboxylato-κ2O,N)cobalt(III) monohydrate, ***Acta Crystallographica Section E***, **61**, 481.
4. Z. Kristallogr, (2011) Crystal structure of (2,2'-bipyridine-" 2N:N')-bis[(DL)-camphorato]- copper(II) dihydrate, Cu(C10H8N2)(C10H15O4)2 2H2O, ***ZNCS***, **226**, 191-192.
5. A. Altomare, M. Cascarano, C. Giacovazzo, A. Guagliardi, (1993) Completion and refinement of crystal structures with SIR92, ***Journal of Applied Crystallography***, **26**, 343-350.
6. G. M. Scheldrink, (2008) A short history of SHELX, *Acta Cryst*, **A64**, 112-124.
7. Bruker AXS Inc., (2004) ***Bruker APEX2, SADABS, XPREP, and SAINT-Plus***, Madison, Wisconsin, USA, Bruker AXS Inc.
8. L. J. Farrugia, (1997) ORTEP-3 for Windows - a version of ORTEP-III with a Graphical User Interface (GUI), ***Journal of Applied Crystallography***, **30**, 565.
9. I. J. Bruno, J. C. Cole, P. R. Edgington, (2002) New software for searching the cambridge structural database and visualizing crystal structures, ***Acta Crystallographica Section B***, **58**, 389-397.
10. V. N. Staroverov, G. E. Scuseria, (2003) Comparative assessment of a new nonempirical density functional: Molecules and hydrogen-bonded complexes, ***Journal of Chemical Physics***, **119**, 12129.
11. E. Van Lenthe, E. J. Baerends, J. G. Snijders, (1994) Rela-tivistic total energy using regular approximations, ***Journal of Chemical Physics,*** **101**, 9783-9792.
12. A. Schafer, C. Huber, R. Ahlrichs, (1994) Fully optimized contracted Gaussian basis sets of triple zeta valence quality for atoms Li to Kr, ***Journal of Chem Physics,*** **100**, 5829.
13. F. Neese, A. Wennmohs, (2009) Hansen. ***Chemical Physics***, **356**, 98.
14. E. M. Sproviero, J. A. Gascón, J. P. McEvoy, (2008) Quantum mechanics/molecular mechanics study of the catalytic cycle of water splitting in photosystem II, ***Journal of American Chemical Society***, **130**, 3428.
15. S. Grimme, S. Ehrlich, L, Goerigk, (2011) Effect of the damping function in dispersion corrected density functional theory, ***Journal of Computational Chemistry***, **32**, 1456-1465.
16. F. Neese, (2018) Software update: The ORCA program system, version 4.0, ***Wires Computational Molecular Science***, **8**, 1327.

17. C. Lee, W. Yang, R. G. Parr, (1988) Development of the Colle-Salvetti correlation-energy formula into a functional of the electron density, ***Physical Review. B, Condensed Matter***, **37**, 785-789.
18. M. A. Spackman, D. Jayatilaka, (2009) Hirshfeld surface analysis, ***CrystEngComm***, **11**, 19-32.
19. Y. He, H. Z. Kou, Y. Li, (2003) One-pot template synthesis and crystal structure of two new polyaza copper(II) complexes, ***Inorganic Chemistry Communications***, **6**, 38.
20. J. W. Shin, S. M. Yeo, K. S. Min. (2012) Copper(II) coordination compounds containing chiral functional groups as pendants: Syntheses, crystal structures, and physical properties, ***Inorganic Chemistry Communications***, **22**, 162.
21. B. Cordero, V. Gomez, A. E. Platero-Prats, M. Revés, J. Echeverría, E. Cremades, F. Barragán, S. Alvarez. (2008) Covalent radii revisited, ***Dalton Trans***, **21**, 2832-2838.
22. P. Pyykko, M. Atsumi, (2009) Molecular double-bond covalent radii for elements li-E112, ***ChemEurJ***, **15**, 86.
23. A. G. Orpen, L. Brammer, F. H. Allen, O. Kennard, D. G. Watson, R. Taylor, (1989) ***Journal of the Chemical Society Dalton Transactions***, **1989**, 12.
24. A. E. Lapshin, O. V. Magdysyuk, (2009) Structure of a biologically active binuclear palladium complex in the compound (bis[(μ2-2-chloroethylammonium)(1,10-phenanthroline)-palladium(I)]) tetranitrates hydrate, ***Glass Physics and Chemistry***, **35**, 627-636.
25. M. Swiatkowski, R. Kruszynski, (2017) Revealing the structural chemistry of the group 12 halide coordination compounds with 2,2′-bipyridine and 1,10-phenanthroline, ***Journal of Coordination Chemistry***, **70**, 642-675.
26. K. Fukui, (1975) ***Theory of Orientation and Stereo Selection***, Berlin: Springer-Verlag.
27. B. R. Chavdaa, (2021) Coordination behavior of dinuclear silver complex of sulfamethoxazole with solvent molecule having static rotational disorder: Spectroscopic characterization, crystal structure, Hirshfeld surface and antimicrobial activity, ***Journal of Molecular Structure***, **1228**, 129777.
28. B. Zurowska, J. Ochocki, J. (2004) Mrozinski, ***Inorgancia Chim Acta Journal***, **3**, 755-763.
29. J. J. McKinnon, D. Jayatilaka, M. A. Spackman, (2007) Towards quantitative analysis of intermolecular interactions with hirshfeld surfaces, ***Chemical Communications,*** **2007**, 3814-3816.
30. F. P. Fabbiani, L. T. Byrne, J. J. Mckinnon, M. A. Spackman, (2007) Solvent inclusion in the structural voids of form II carbamazepine: Single-crystal X-ray diffraction, NMR spectroscopy and Hirshfeld surface analysis, ***CrystEngComm,*** **9**, 728-731.
31. J. J. McKinnon, M. A. Spackman, A. S. Mitchell, (2004) Novel tools for visualizing and exploring intermolecular interactions in molecular crystals, ***Acta Crystallogr B***, **60**, 627-668.

Bibliographical Sketch

Dr. Vikas Kumar Dakua is a Associate Professor of Organic Chemistry, Alipurduar University, India. His Present Research interests include synthesis of Metal-Organic Hybrid Materials. He also works on Solution Thermodynamics and Nano Chemistry. At present He has 30 research articles published in various peer reviewed national and international journals. Amid these articles, 14 research articles are h-indexed. He has been a reviewer of some journal, Elsevier, Springer. He has already supervised one research Scholar for the PhD and two scholars are presently pursuing their PhD under his Co-supervision.